



**HAL**  
open science

## Online reaction monitoring with fast and flow-compatible diffusion NMR spectroscopy

Achille Marchand, Rituraj Mishra, Aurélie Bernard, Jean-nicolas Dumez

### ► To cite this version:

Achille Marchand, Rituraj Mishra, Aurélie Bernard, Jean-nicolas Dumez. Online reaction monitoring with fast and flow-compatible diffusion NMR spectroscopy. *Chemistry - A European Journal*, In press, 10.1002/chem.202201175 . hal-03765236

**HAL Id: hal-03765236**

**<https://hal.science/hal-03765236>**

Submitted on 31 Aug 2022

**HAL** is a multi-disciplinary open access archive for the deposit and dissemination of scientific research documents, whether they are published or not. The documents may come from teaching and research institutions in France or abroad, or from public or private research centers.

L'archive ouverte pluridisciplinaire **HAL**, est destinée au dépôt et à la diffusion de documents scientifiques de niveau recherche, publiés ou non, émanant des établissements d'enseignement et de recherche français ou étrangers, des laboratoires publics ou privés.

# Online reaction monitoring with fast and flow-compatible diffusion NMR spectroscopy

Achille Marchand, Rituraj Mishra, Aurélie Bernard, Jean-Nicolas Dumez\*

[a] A. Marchand, Dr R. Mishra, A. Bernard, Dr J.-N. Dumez  
Nantes Université, CNRS, CEISAM UMR 6230, F-44000 Nantes, France  
E-mail: jean-nicolas.dumez@univ-nantes.fr

Supporting information for this article is given via a link at the end of the document

**Abstract:** Online monitoring by flow NMR spectroscopy is a powerful approach to study chemical reactions and processes, which can provide mechanistic understanding, and drive optimisations. However, some of the most useful methods for mixture analysis and reaction monitoring are not directly applicable in flow conditions. This is the case of classic diffusion-ordered NMR spectroscopy (DOSY) methods, which can be used to separate the spectral information for mixture's components. We describe a fast and flow-compatible diffusion NMR experiment that makes it possible to collect accurate diffusion data for samples flowing at up to 3 mL/min. We use it to monitor the synthesis of a Schiff base with a flow-tube with a time resolution of approximately 2 minutes. The one-shot flow-compatible diffusion NMR described here opens many avenues for reaction monitoring applications.

## Introduction

Reaction monitoring by NMR spectroscopy provides unique chemical insight.<sup>[1–3]</sup> Online monitoring by flow NMR is a powerful method that makes it possible to analyse reactions carried out in relevant experimental conditions.<sup>[4–11]</sup> It has notably been shown that reaction kinetics as measured in an NMR tube may not be representative of what happens in a round-bottomed flask with stirring.<sup>[12]</sup> Flow NMR also makes it easier to, e.g., use external stimuli or add reactants during the course of a reaction. Online monitoring is achieved by creating a loop of reaction medium that goes from the benchwork to the magnet and back.<sup>[4–6,8]</sup> The sample flow, however, has consequences for NMR experiments, such as the so-called “in-flow” and “out-flow” effects on quantification.

Reaction monitoring by NMR is most often performed with pulse-acquire experiments. The complexity of the resulting spectra, can be an obstacle. Diffusion-ordered spectroscopy (DOSY) is a powerful tool to analyse complex mixtures by NMR, as it makes it possible to separate the spectra of a mixture's components. The relevance of DOSY for reaction monitoring has been clearly illustrated with, e.g., the detection of species presents during amyloid fibril formation<sup>[13]</sup>. The diffusion coefficients measured by NMR can themselves be of high interest, as shown by a recent controversy on the existence, or not, of “boosted mobility” in chemical reactions of small organic molecules.<sup>[14–16]</sup> Moreover, diffusion coefficients provide information such as size,<sup>[17]</sup> aggregation,<sup>[18]</sup> solvent interaction,<sup>[19]</sup> encapsulation.<sup>[20]</sup> DOSY experiments rely on a diffusion-induced signal attenuation that results from the application of pulsed magnetic-field gradients, and on the acquisition of several consecutive sub-experiments with different gradient intensities. Recent examples of DOSY experiments in the context of online monitoring by flow NMR relied on a stopped-flow acquisition,<sup>[21]</sup> and to our knowledge such methods were never used on flow.

Measuring diffusion coefficients in flow conditions may seem counter-intuitive. Pulsed-field gradients give additional effects

when molecules experience motions other than diffusion within the sample. This is typically the case when temperature gradients cause sample convection. Several methods have been developed to compensate for the effect of convection, such as the use of double diffusion-encoding schemes,<sup>[22]</sup> and that of transverse diffusion-encoding gradients.<sup>[23,24]</sup> Another important consideration is that the time requirement of conventional DOSY experiments sets a limit on the accessible reaction timescales. DOSY experiments may notably be accelerated by reducing the number of scans to 1 per gradient increment,<sup>[25,26]</sup> by randomization of the sampled gradient intensities,<sup>[27]</sup> and by spatial parallelization,<sup>[28]</sup> and again these methods were to our knowledge never used on flow.

In this article, we show that DOSY data can be collected for online monitoring by flow NMR with surprising accuracy. Using a commercially available flow-tube and a triple-axis gradient probe, we describe pulse sequences that employ double-diffusion encoding along a transverse axis to yield accurate diffusion coefficients, for samples flowing at up to 3 mL/min. We also show how, using optimized coherence selection gradients, the duration of each experiment can be reduced to less than 90 s, while preserving good accuracy. The resulting one-shot DSTE DOSY method is fast (~80 s) and flow compatible. We use it for the online monitoring of diffusion coefficients throughout the synthesis of a Schiff base. These results open perspectives for the “unmixing” of spectra for reaction mixtures monitored by flow NMR, as well as investigations of interactions and mobility during chemical reactions

## Accurate diffusion experiments in flow conditions

DOSY experiments rely on a pair of magnetic-field gradient pulses separated by a delay. Diffusion during the delay results in an attenuation of the form<sup>[29]</sup>:

$$(1) \quad \frac{S}{S_0} = \exp(-D\Delta'(\gamma\sigma G\delta)^2)$$

where  $D$  is the translational diffusion coefficient,  $\Delta'$  is the diffusion delay corrected to account for finite pulse width,  $\gamma$  is the gyromagnetic ratio of the nuclei involved,  $G$  is the amplitude of the gradient pulses with  $\delta$  duration, and  $\sigma$  is the shape factor. Usually, a series of spectra is acquired for different values of  $G$ . DOSY processing then consists of fitting the decay of peaks integrals to equation (1) to yield an estimate of the diffusion coefficient of the molecules from which that peak originates.

The most commonly used DOSY pulse sequence is based on a pair of bipolar gradient pulses separated by a diffusion delay. A stimulated echo (STE) is used to minimise the effect of nuclear spin relaxation and signal distortion due to J-evolution<sup>[30]</sup>. The

## RESEARCH ARTICLE

STE pulse sequence used here is shown in Figure 1a. A special feature of this sequence is the use of different gradient axes for diffusion-encoding and for coherence transfer pathway (CTP) selection, as will be discussed in next section. In this section phase cycling is used for CTP selection. A LED (longitudinal Eddy Current) block<sup>[31]</sup> was not used here, as it was not found to have any benefits with our hardware. A triple-axis gradient probe is used here, and the possibility to apply magnetic field gradient pulses along several axes is essential for the reported method.

NMR experiments were carried out with non-deuterated solvents, since deuteration can influence reaction kinetics and diffusion coefficients, and since the cost of large volumes of deuterated solvents would be prohibitive. The WET (Water suppression enhanced through T<sub>1</sub> effects)<sup>[32]</sup> block was selected here to suppress the solvent signal, as it is known to be efficient on a flowing sample, and can be adapted to suppress multiple solvent peaks. The use of different gradient axes for diffusion encoding and solvent suppression is an efficient solution to achieve adequate solvent suppression.

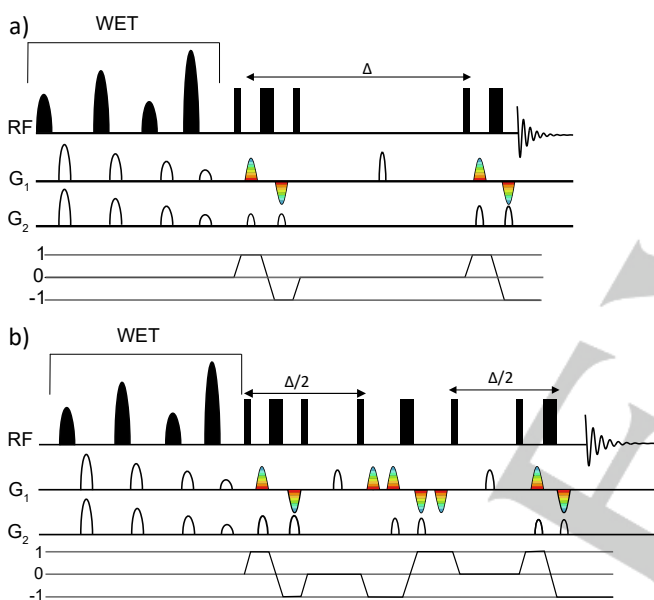


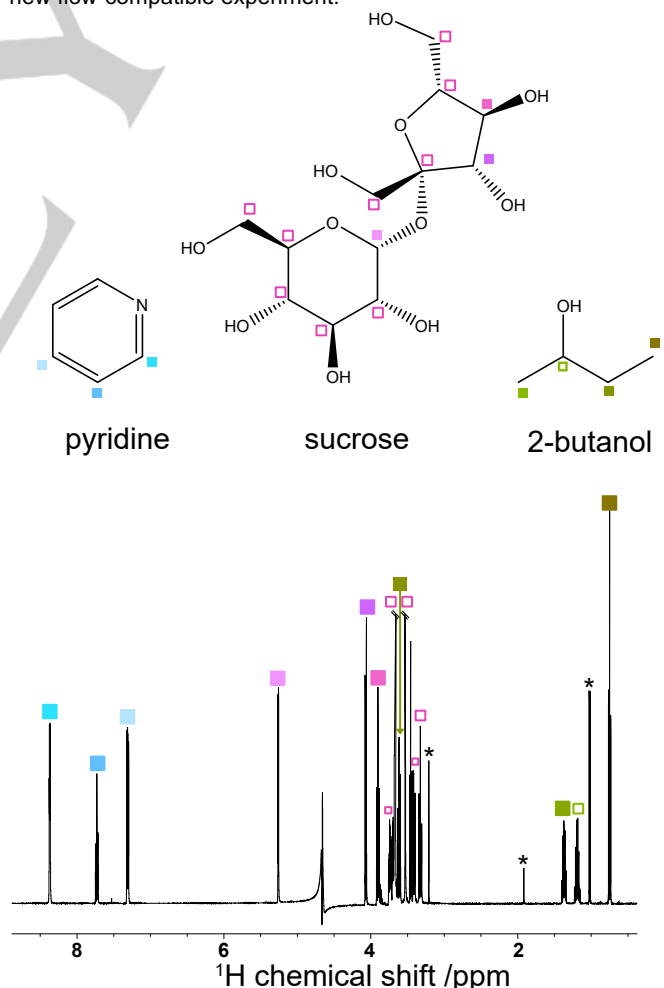
Figure 1: Pulse sequences for DOSY NMR. Narrow black rectangle corresponds to 90° pulses, large ones correspond to 180° pulses. Black half ellipses correspond to selective pulse targeting the solvent signal, as described in Ref. 21. White half ellipses correspond to magnetic-field gradient pulses, which may be applied along two different axes. Rainbow half ellipses correspond to incremented magnetic-field gradient pulses. Additional gradient pulses (not shown) are also included to ensure a total gradient integral of zero for each scan. The selected coherence transfer pathway is shown under each pulse sequence. a) Stimulated-echo (STE) pulse sequence with orthogonal coherence-selection gradients and WET solvent suppression. b) Double stimulated-echo (DSTE) pulse sequence with orthogonal coherence-selection gradients and WET solvent suppression. Note that while G1 and G2 correspond to different tasks, they may be applied either on the same physical axis or on different physical axes.

A first objective is to characterise, and mitigate, the effect of the sample flow on DOSY experiments. This was achieved with the model sample shown in Figure 2, consisting of three small molecules at a concentration of 100 mM in non-deuterated water. The sample was flown at 3 mL/min, a <sup>1</sup>H 1D spectrum acquired in flow conditions is shown in Figure 2. Three well resolved peaks

were selected for each compound, and analysed for a series of experiments.

Flow within the tube is expected to interfere with diffusion encoding. This can be understood in two steps. First, when a pair of gradients separated by a delay is applied, if the velocity of a volume element is non-zero along this gradient axis, then the magnetization of that volume element will acquire a phase shift.<sup>[33]</sup> Then, since in the flowtube a distribution of velocities is present, there is overall a distribution of phase shifts and hence the signal decays/oscillates. Note that the flow distribution within the flowtube is expected to be laminar<sup>[6]</sup>. At a flow rate of 3 mL/min the average linear velocity is approximately 3 mm/s, resulting in a Reynolds number of 15 for water and 30 for acetonitrile at 298 K.

Flow effects will result in a systematic error of the estimated diffusion coefficients for classic DOSY pulse sequences. It will also result in a larger estimated uncertainty (which translates as the width of the peak in the diffusion dimension in DOSY spectra), because the experimental signal decays will not be suitably described by Equation (1). As expected, DOSY experiments recorded with longitudinal (z) diffusion encoding and a STE pulse sequence for a flowing sample yields poor results, as shown in Figure 3. The measured diffusion coefficients are overestimated by 100 % (compared to reference values acquired with a STE pulse sequence in static conditions in the flowtube, out-of-flow), and the peaks are very large in the diffusion dimension, with a width of more than  $2 \times 10^{-10}$  m<sup>2</sup>/s, versus  $0.15 \times 10^{-10}$  m<sup>2</sup>/s for the new flow-compatible experiment.



## RESEARCH ARTICLE

Figure 2: Molecules present in the test sample and their solvent-suppressed 1D  $^1\text{H}$  spectrum in non-deuterated water. Filled squares indicate the peaks used to evaluate DOSY pulse sequences. Note that isopropanol is present as an impurity as a result of cleaning/storing the flow tube.

Several metrics are used to assess the quality of the data, and shown in Figure 3a and 3b. The position of each point is given by the estimated diffusion coefficient averaged over the three selected peaks for each molecule. The associated error bar is

calculated in two different ways. In Figure 3a, the error bar is chosen to represent the root-mean-square of the peak's vertical width for the three selected peaks. It is a measure of the "resolution" in the DOSY display. In Figure 3b, the error bar is calculated, for each molecule, as the standard deviation for the three values corresponding to three selected peaks. It is thus a measure of the inconsistency between diffusion coefficient values from one peak to another in a given molecule. A high-quality DOSY experiment should minimize these two types of errors. The STE sequence with longitudinal encoding fails on all accounts in flow.

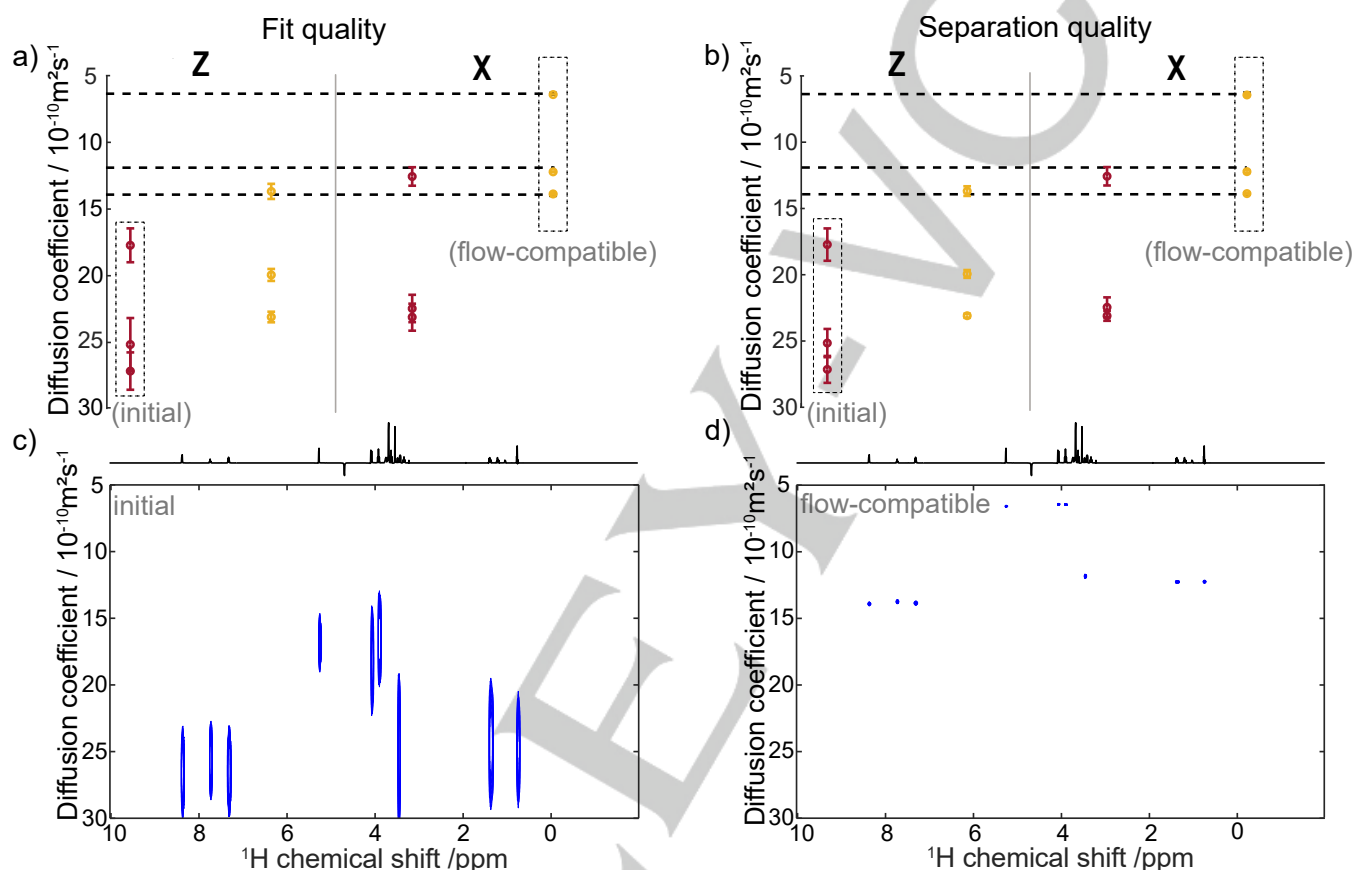


Figure 3: Diffusion coefficients measured with DOSY pulse sequences in flow conditions. In a) and b), the position of each data point corresponds to the measured diffusion coefficient for a molecule in sample A averaged over three different peaks. For some series error bars are too small to be seen. Reference values, measured with STE DOSY in the absence of flow in the flow tube, are shown as a dotted line. Values obtained with STE DOSY are shown in red, and values obtained with DSTE DOSY are shown in yellow. The diffusion encoding axis is either longitudinal (Z) or transverse (X), as indicated on the figure. In a), error bars correspond to the error calculated by the fit. In b), error bars correspond to standard deviation among the diffusion coefficient for the same molecule. c) DOSY spectrum obtained with the STE pulse sequence using longitudinal diffusion-encoding gradients. d) DOSY spectrum obtained with a DSTE pulse sequence using transverse diffusion-encoding gradients.

The problem of dealing with displacements of volume elements during DOSY experiments has been addressed in the case of convection, in two different ways. A first approach is to use two diffusion-encoding steps instead of one, with coherence transfer pathways chosen such that the effect of velocity on the detected signal is compensated, while the effect of diffusion is cumulative. The double stimulated echo pulse (DSTE) sequence was thus designed to "refocus all constant velocity effects"<sup>[22]</sup>. A second approach is to use a diffusion-encoding gradient that is orthogonal to the main direction of the flow<sup>[33]</sup>. We will refer to this second approach as transverse diffusion encoding, since the flow is mainly along z in our setup. Here we tested the two methods,

and the results are summarised in Figure 3. Remarkably, thanks to a combination of transverse encoding and double-diffusion encoding, the new flow-compatible DOSY pulse sequence yields accurate values of the diffusion coefficients, that differ by less than 2 % from the values measured in the absence of flow. Neither transverse encoding nor double-diffusion encoding alone did achieve this result, as shown in Figure S1.

The velocity distribution in the flow-tube has not been mapped in detail as it was not required to monitor the reaction. The results described here show that the z component of the velocity does not meet the requirement of being "constant", leading to the failure of the DSTE sequence when diffusion is encoded along z. On the

## RESEARCH ARTICLE

other hand, the transverse component of the velocity is not negligible either, since transverse diffusion encoding also fails to give exact diffusion coefficients with the STE sequence.

## One-shot DOSY in flow condition

The duration of conventional DOSY experiments is an obstacle for reaction monitoring applications. It results from: i/ the requirement to sample several gradient values, usually between 8 and 32; ii/ the relaxation delay between consecutive scans; iii/ the use of phase cycling for CTP selection, which gives a minimum of 8 scans per gradient increment for the STE sequence, and 16 for the DSTE sequence. Methods have been reported to address these three points.<sup>[27,28,34]</sup>

Here we first worked on reducing the number of scans per increment to 1, by using additional gradient pulses for CTP selection. Experiments were first carried out in the absence of flow, on a model sample placed in a standard 5 mm tube, with the pulse sequences shown in Figure 1, and the results are summarised in

Figure 4. When a single-gradient axis is available, CTP selection gradients are necessarily parallel to the diffusion-encoding gradient. This possibility was first described by Pelta et al.<sup>[26]</sup> and further documented by Guest.<sup>[35]</sup> It can be seen in Figure 4 for the STE sequence that in this case, the measured diffusion coefficients are systematically underestimated, compared to the results obtained with phase cycling. When several gradient axes are available, orthogonal axes may be used for diffusion encoding and CTP selection.<sup>[25]</sup> As shown in Figure 4, this improves both the accuracy of the estimated diffusion coefficients, and the width of the peaks in the diffusion dimension.

The use of a single-scan per increment instead of  $n$  scans (with  $n > 1$ ) results in a decrease of SNR by a factor of  $\sqrt{n}$  following the usual dependence of sensitivity on the number of scans. Since SNR can also influence the quality of DOSY experiments, experiments carried out with 8 averaged scans per increment but without phase cycling were performed and confirm that the observed errors are due to imperfect CTP selection rather than sensitivity, as shown in Figure 4.

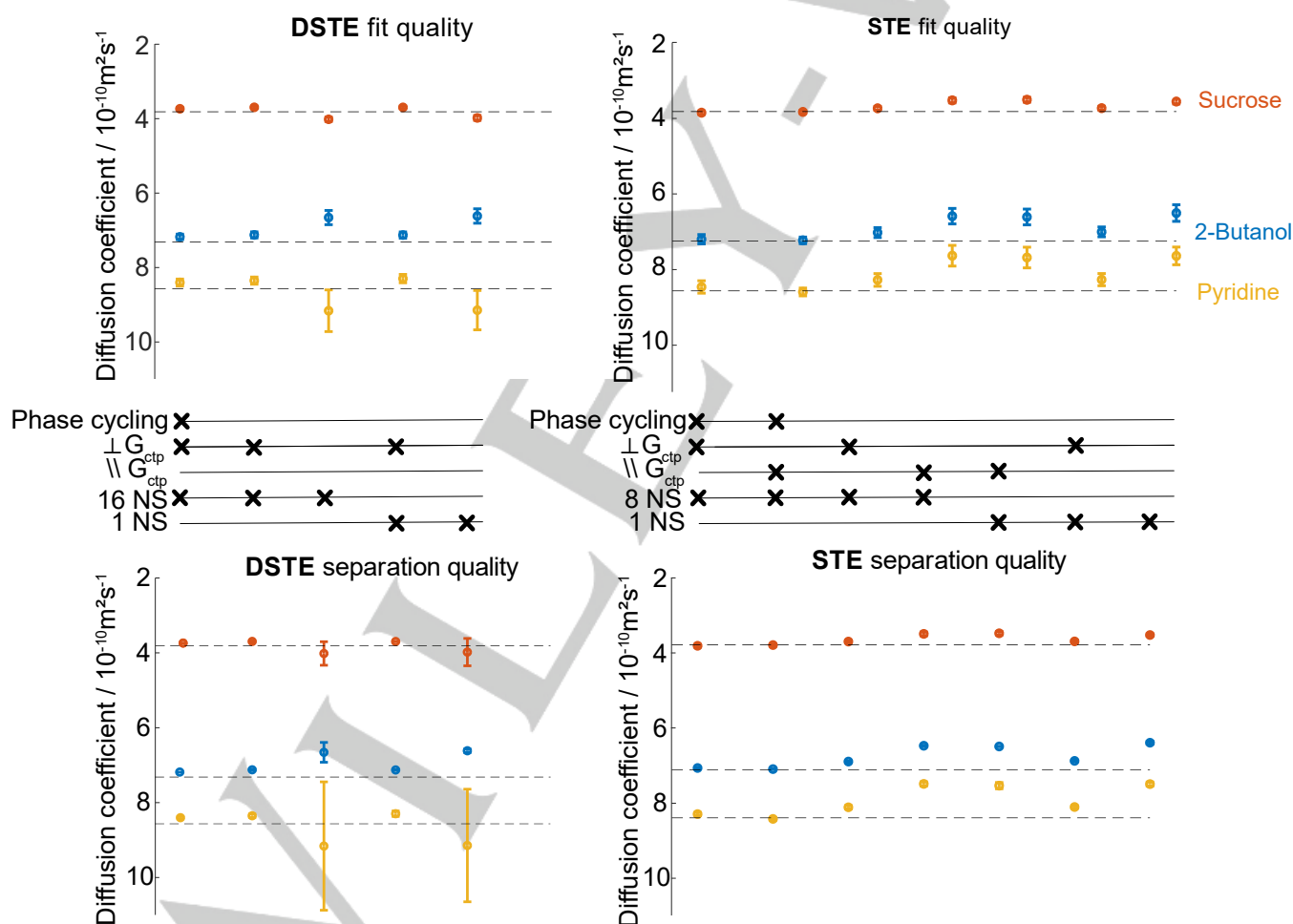


Figure 4: Diffusion coefficients measured with different coherence selection schemes, with the STE (right) and DSTE (left) pulse sequences shown in Figure 1. Reference values, measured with STE DOSY and a 8-step phase cycle, are shown with dotted lines. For some series (especially STE separation here) error bars are too small to be seen. The use of phase cycling, parallel coherence-selection gradients ( $\parallel G_{\text{ctp}}$ ), and orthogonal coherence selection gradients ( $\perp G_{\text{ctp}}$ ) is indicated for each experiment, together with the number of scans, and the use or not of phase cycling. The two left panels refer to DSTE experiments without flow. The two right panels refer to STE experiments without flow. In the two top panels, the error bar corresponds to the error as calculated by the fit. In the two bottom panels, error bars correspond to standard deviation among coefficient for the same molecule. All experiment displayed here are out-of-flow. All DOSY plots are available in SI.

## RESEARCH ARTICLE

Similar results are obtained with the DSTE sequence. In the absence of CTP selection there are significant differences between the estimated diffusion coefficients and the reference values, as well as larger peaks in the diffusion dimension. When orthogonal CTP-selection gradients are used, the estimated diffusion coefficients differ by less than 3% from the reference values, and the width of the peak is comparable to that obtained with phase cycling. This is, to the best of our knowledge, the first example of a “one-shot” DSTE DOSY pulses sequence, i.e., with a single scan per gradient increment

The one-shot DSTE pulse sequence was also tested for a sample flowing at 3 mL/min. Their resulting DOSY spectrum, shown in Figure 5, demonstrates that high-quality DOSY data can be obtained by flow NMR, with a total experimental time of just 80 s. This opens the possibility to use DOSY for online monitoring in flow conditions.

### Online monitoring

As an illustration of online monitoring by DOSY flow NMR, we chose to monitor the di-imerization reaction shown in Figure 6a, carried out in acetonitrile. The reaction was carried out in a round-bottomed flask, and monitored with a commercial flow tube and peristaltic pump, with a flow rate of 3 mL/min. The evolution of the reaction mixture was monitored by the acquisition of DOSY spectra every 2 min, with each DOSY experiment lasting 80 s. A representative 1D spectrum for the reaction mixture is shown in Figure 6b.

The time evolution of peak integrals from the time series of DOSY experiments is shown in Figure 6c. They were obtained by peak integration in the least attenuated increment (see Figure S7). In this reaction, a mono-imine intermediate is first formed. In the present conditions, its concentration reaches a maximum after 84 min. If DSTE experiments were used with phase cycling, the time resolution would result in only four points before this maximum. The estimated diffusion coefficients obtained with the one-shot DSTE sequence during the course of the reaction are shown in Fig 6. In this reaction, no change in diffusion coefficient is expected over time for a given species, and it can be used to validate the measurement methods. For signals with SNR larger than ~200, the estimated diffusion coefficients for each peak are found to have a relative variation of less than 2% on average, the maximum difference between the estimated diffusion coefficients for two different peaks of the same molecule at a given time point is of about 10%. The diffusion coefficients of the two reactants have also been measured separately, in the same solvent and at same concentration. The average diffusion coefficients measured during the reaction differ from those measured on non-reacting samples by less than 5%.

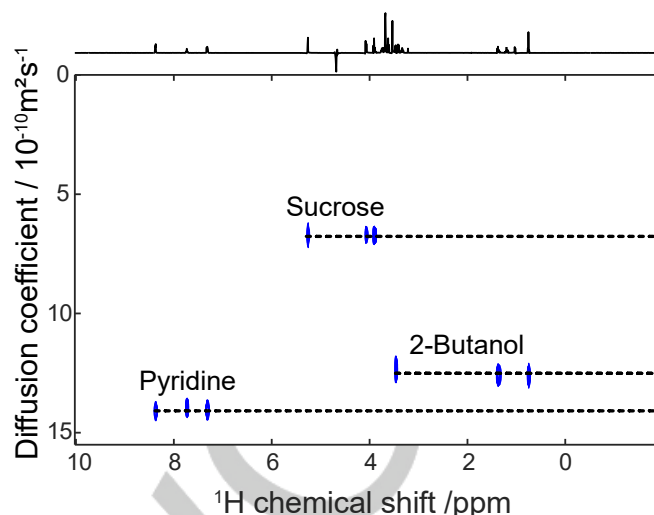


Figure 5 : DOSY spectrum for selected peaks in a sample of sucrose, 2-butanol and pyridine in water, acquired with a flow rate of 3 mL/min with 1scan per increment (total experiment time 90s).

Signals that have insufficient SNR are not expected to yield accurate values of diffusion coefficients. In this case, for a reaction time of less than 50 min, the di-imine is not present or its concentration is too low. As a result, the resulting coefficients show larger estimated errors. Also, five signals (including the water signal) in the spectrum cannot be integrated reliably, because of signal overlap, chemical exchange, proximity to the solvent signals, and low SNR due to high multiplicity. These are indicated with empty squares on Figure 6b. Still, DOSY processing can yield partial separation of the compound's spectra, as shown in Figure 7.

The results shown in Figures 6 and 7 give an indication of the accuracy of the proposed flow DOSY method. Time-resolved measurement of diffusion coefficients have been shown to be a powerful approach to separate the spectra of components in a reactive mixture, notably by multivariate processing<sup>[36]</sup>. The described method should make it possible to use this approach for online monitoring by flow NMR.

It can be noted that the relative intensities reported in Figure 6 may be translated into absolute intensities by calibration. In the case of the reactant, this is straightforward since the initial concentration is known. In the case of other species, calibration would require measurement on a purified compound, or a calculation that accounts for relaxation, flow, and diffusion effects.

The use of a fast DOSY experiment has several additional advantages. First, the time resolution that can be achieved becomes closer to that of the 1D <sup>1</sup>H NMR that are typically used to monitor changes in concentrations, and the two experiments can be simply interleaved. The best achievable time resolution will depend on the sample's concentration. If the SNR of one-shot experiments is insufficient, signal averaging can be used to achieve a compromise between sensitivity and time resolution. Second, since experiments with non-deuterated solvents are more susceptible to changes in the magnetic field homogeneity and field drift, shorter experiments also make it possible to interleave routine shimming to adjust the field homogeneity. Routine shim experiments can be seen in Figure 6c as small gaps between experiments.

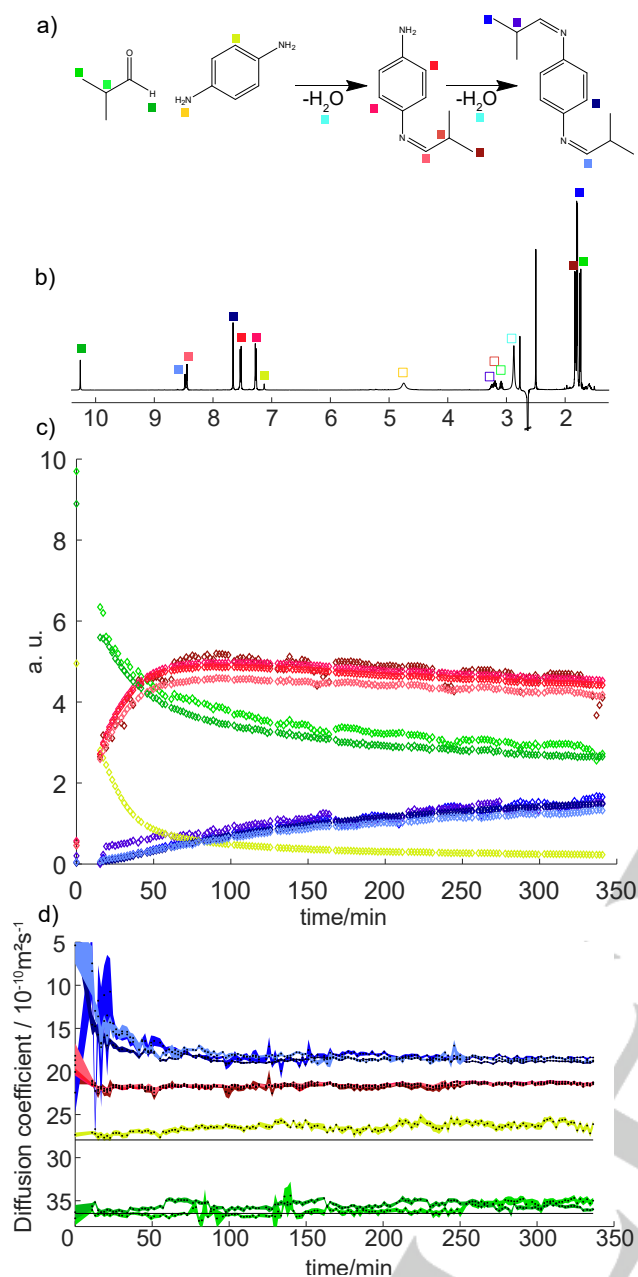


Figure 6: Reaction monitoring by flow DOSY NMR. a) Scheme of the di-imination reaction monitored by online NMR at a flow rate of 3 mL/min. b) 1D  $^1\text{H}$  NMR spectrum of the reaction mixture. Coloured squares are used to assign the peaks. In b) empty squares are used for peak that cannot be reliably integrated (see text above). c) Time evolution of the peak integrals in the DOSY increment with minimum diffusion attenuation acquired on flow (corrected for the number of protons per site). Integration regions are shown in Figure S7. d) Time evolution of the measured diffusion coefficients. The width of the curve corresponds to the uncertainty estimated from the fit. The black line corresponds to reference values for the reactants, measured on a non-reacting sample and in the absence of flow.

Diffusion NMR data is most often acquired with a list of gradient values that are in increasing order. However, when concentrations of the compounds are changing over time, any correlation between chemical change and the degree of diffusion attenuation will result in a biased estimate of the diffusion coefficients. This was notably documented by Oikonomou et al.<sup>[37]</sup>, who showed that using a list of permuted gradient values made

it possible to avoid this bias. The data shown in Figure 6c shows that concentrations change by up to 7% during the course of an 80 s acquisition. We chose to use permuted gradient lists, to avoid any bias. Note that the time resolution could be further improved by using a list of long pseudo-random gradient values, together with a sliding-window processing, in the so-called time-resolved DOSY approach<sup>[27,38]</sup>.

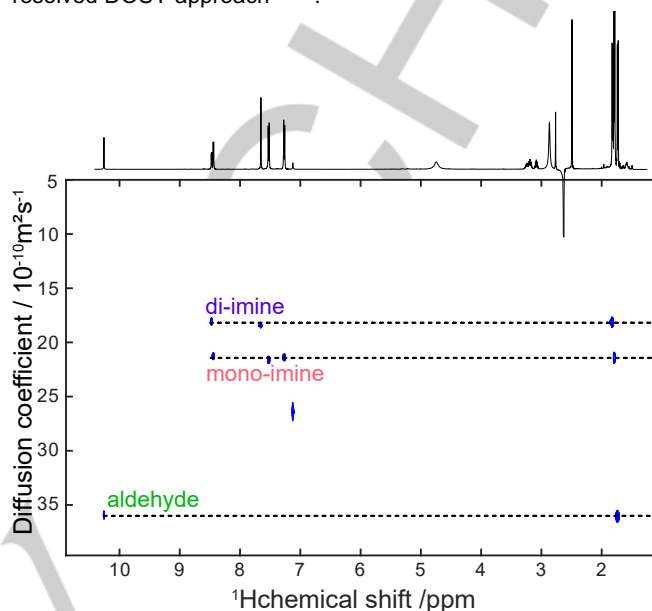


Figure 7 : DOSY spectrum of reaction medium in flow for selected peak. Flow is 3mL/min total time of the experiment was 80s.

## Conclusion

We have shown that diffusion-ordered spectroscopy can be used for online reaction monitoring by flow NMR, with a time resolution of just two minutes, which is relevant for a broad range of reactions. DOSY and 1D experiments can be interleaved to collect information on both concentrations and diffusion coefficients. Fast flow DOSY NMR requires the use of pulse sequences that address velocity effects on diffusion measurements, and coherence-selection schemes that are optimised to collect only one scan per gradient increment. The implementation of this method is straightforward, provided that a triple-axis gradient probe is available. The method opens several avenues for the applications in reaction monitoring, including the unmixing of spectra of products in a reaction, and the monitoring of changes in diffusion coefficients in fields such as polymer and supramolecular chemistry.

## Experimental Section

All the experiments were carried out on a Bruker Avance III spectrometer operating at a  $^1\text{H}$  Larmor frequency of 500.13 MHz, using an inverse-detection probe equipped with triple-axis gradients, at a nominal temperature of 298K. The gradient coil delivers a maximum of 47 G/cm on each transverse axis and 63 G/cm on the longitudinal axis.

Flow NMR experiments were carried out using a commercial 7m long flow tube (InsightMR, Bruker) for 5 mm probes, using a

PEEK capillary and a Vapourtec SF-10 peristaltic pump. All the flow experiments were carried out with a flow rate of 3 ml/min in an air-conditioned room.

Sample A consisted of a mixture of sucrose, 2-butanol and pyridine in 600  $\mu$ l of D<sub>2</sub>O. The resulting sample concentration was 100 mmol/L for each compound. An equivalent sample was prepared in 30 ml of H<sub>2</sub>O (non-deuterated), at the same concentrations, for flow studies.

Sample B consisted of a reaction mixture, prepared as follows. First, 256 mg of p-phenylenediamine were dissolved into 30 ml of acetonitrile (1Eq). The reaction medium was stirred under a fumehood until complete solubilization. It was then flowed through the flowtube for online monitoring (to the magnet and back). 0.42 ml of aldehyde (2Eq) was then added to the flask under stirring, using a syringe (Hamilton).

DOSY experiments were acquired with an acquisition time of 1.36 s for sample A and 0.74 s for sample B, an inter-scan delay of 3 seconds and 4 dummy scans. The gradient list consisted of 16 increments that form a linear grid from 10% to 80% of the maximum gradient strength. For experiments on sample A, the diffusion-encoding parameters were  $\Delta = 0.16$  s and  $\delta = 1.4$  ms. For monitoring experiments, the diffusion-encoding parameters were  $\Delta = 0.10$  s and  $\delta = 0.8$  ms. The number of scans per increment ranged from 1 to 16, resulting in a total duration ranging from 80 s to 20 min for DOSY experiments. <sup>1</sup>H 1D experiment using WET solvent suppression were interleaved during reaction monitoring to monitor changes of the field homogeneity or other possible issues.

For reaction monitoring, the gradient values in the list were randomly permuted to avoid interferences from the raising and lowering of species concentration.<sup>[37]</sup>

All the spectra were first processed with the Topspin software (Bruker) for zero filling and apodization, Fourier transform, phasing and baseline correction. For integration of the peaks, the data were imported in MATLAB thanks to the RBNMR package, and integrated with custom scripts from the increment of each DOSY with the lowest diffusion-encoding gradient. For DOSY analysis, the data were imported and analysed with the GNAT<sup>[39,40]</sup> package for peaks integrations, data fitting using monoexponential fitting, and display.

## Acknowledgements

The authors thank Patrick Giraudeau for useful discussions and comments on the manuscript and Corentin Jacquemmoz for his contribution on the flow-assembly. This work has received funding from the European Research Council (ERC) under the European Union's Horizon 2020 research and innovation program (grant agreements no 801774/DINAMIX) and the Region Pays de la Loire (Connect Talent HPNMR). The authors also acknowledge the French National Infrastructure for Metabolomics and Fluxomics MetaboHUB-ANR-11-INBS-0010 ([www.metabohub.fr](http://www.metabohub.fr)) and the Corsaire metabolomics core facility (Biogenouest).

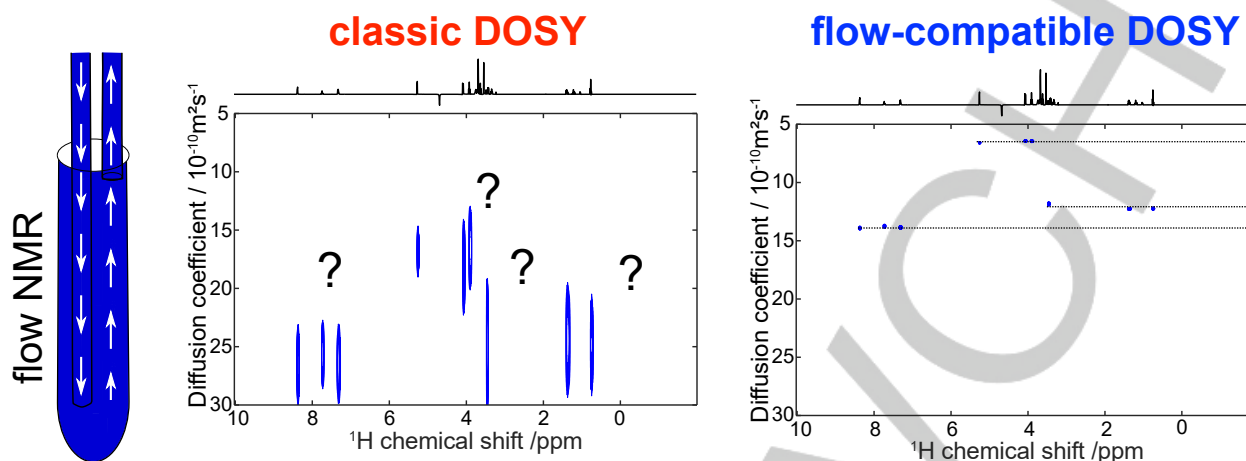
**Keywords:** NMR spectroscopy • Analytical methods • diffusion NMR • DOSY • online monitoring • flow NMR

[1] Y. Ben-Tal, P. J. Boaler, H. J. A. Dale, R. E. Dooley, N. A. Fohn, Y. Gao, A. Garcia-Dominguez, K. M. Grant, A. M. R. Hall, H. L. D. Hayes, M. M. Kucharski, R. Wei, G. C. Lloyd-Jones, *Prog. Nucl. Magn. Reson. Spectrosc.* **2022**, *129*, 28-106.

- [2] M. H. Haindl, J. Hioe, R. M. Gschwind, *J. Am. Chem. Soc.* **2015**, *137*, 12835–12842.
- [3] G. Hutchinson, C. Alamillo-Ferrer, J. Burés, *J. Am. Chem. Soc.* **2021**, *143*, 6805–6809.
- [4] M. Khajeh, M. A. Bernstein, G. A. Morris, *Magn. Reson. Chem.* **2010**, *48*, 516–522.
- [5] D. A. Foley, E. Bez, A. Codina, K. L. Colson, M. Fey, R. Krull, D. Pirolì, M. T. Zell, B. L. Marquez, *Anal. Chem.* **2014**, *86*, 12008–12013.
- [6] A. M. R. Hall, J. C. Chouler, A. Codina, P. T. Gierth, J. P. Lowe, U. Hintermair, *Catal. Sci. Technol.* **2016**, *6*, 8406–8417.
- [7] A. M. R. Hall, R. Broomfield-Tagg, M. Camilleri, D. R. Carbery, A. Codina, D. T. E. Whittaker, S. Coombes, J. P. Lowe, U. Hintermair, *Chem. Commun.* **2018**, *54*, 30–33.
- [8] A. Saib, A. Bara-Estaún, O. J. Harper, D. B. G. Berry, I. A. Thomlinson, R. Broomfield-Tagg, J. P. Lowe, C. L. Lyall, U. Hintermair, *React. Chem. Eng.* **2021**, *6*, 1548–1573.
- [9] A. M. R. Hall, P. Dong, A. Codina, J. P. Lowe, U. Hintermair, *ACS Catal.* **2019**, *9*, 2079–2090.
- [10] A. Martínez-Carrión, M. G. Howlett, C. Alamillo-Ferrer, A. D. Clayton, R. A. Bourne, A. Codina, A. Vidal-Ferran, R. W. Adams, J. Burés, *Angew. Chem. Int. Ed.* **2019**, *58*, 10189–10193.
- [11] M. S. Anwar, C. Hilty, C. Chu, L.-S. Bouchard, K. L. Pierce, A. Pines, *Anal. Chem.* **2007**, *79*, 2806–2811.
- [12] D. A. Foley, A. L. Dunn, M. T. Zell, *Magn. Reson. Chem.* **2016**, *54*, 451–456.
- [13] K. S. Jensen, S. Linse, M. Nilsson, M. Akke, A. Malmendal, *J. Am. Chem. Soc.* **2019**, *141*, 18649–18652.
- [14] J.-P. Günther, L. L. Fillbrook, T. S. C. MacDonald, G. Majer, W. S. Price, P. Fischer, J. E. Beves, *Science* **2021**, *371*, eabe8322.
- [15] N. Rezaei-Ghaleh, J. Agudo-Canalejo, C. Griesinger, R. Golestanian, *J. Am. Chem. Soc.* **2022**, *144*, 1380–1388.
- [16] T. S. C. MacDonald, W. S. Price, R. D. Astumian, J. E. Beves, *Angew. Chem. Int. Ed.* **2019**, *58*, 18864–18867.
- [17] M. D. Christianson, E. H. P. Tan, C. R. Landis, *J. Am. Chem. Soc.* **2010**, *132*, 11461–11463.
- [18] H. B. Jang, H. S. Rho, J. S. Oh, E. H. Nam, S. E. Park, H. Y. Bae, C. E. Song, *Org. Biomol. Chem.* **2010**, *8*, 3918.
- [19] Z. Lyu, F. Yue, X. Yan, J. Shan, D. Xiang, C. M. Pedersen, C. Li, Y. Wang, Y. Qiao, *Fuel Process. Technol.* **2018**, *171*, 117–123.
- [20] L. Avram, Y. Cohen, *Chem. Soc. Rev.* **2015**, *44*, 586–602.
- [21] J. H. Vrijsen, I. A. Thomlinson, M. E. Levere, C. L. Lyall, M. G. Davidson, U. Hintermair, T. Junkers, *Polym. Chem.* **2020**, *11*, 3546–3550.
- [22] A. Jerschow, N. Müller, *J. Magn. Reson.* **1997**, *125*, 372–375.
- [23] C. Jacquemmoz, F. Giraud, J.-N. Dumez, *Analyst* **2020**, *145*, 478–485.
- [24] P. Kiraly, I. Swan, M. Nilsson, G. A. Morris, *J. Magn. Reson.* **2016**, *270*, 24–30.
- [25] R. Sarkar, D. Moskau, F. Ferrage, P. R. Vasos, G. Bodenhausen, *J. Magn. Reson.* **2008**, *193*, 110–118.
- [26] M. D. Pelta, G. A. Morris, M. J. Stchedroff, S. J. Hammond, *Magn. Reson. Chem.* **2002**, *40*, S147–S152.
- [27] T. S. C. MacDonald, W. S. Price, J. E. Beves, *ChemPhysChem* **2019**, *20*, 926–930.
- [28] Y. Shrot, L. Frydman, *Journal of Magnetic Resonance* **2008**, *195*, 226–231.
- [29] E. O. Stejskal, J. E. Tanner, *Chem. Phys.* **1965**, *42*, 288–292.
- [30] J. E. Tanner, *Chem. Phys.* **1970**, *52*, 2523–2526.
- [31] C. S. Johnson, *Prog. Nucl. Magn. Reson. Spectrosc.* **1999**, *34*, 203–256.
- [32] R. J. Ogg, R. B. Kingsley, J. S. Taylor, *J. magn. reson., Ser. B* **1994**, *104*, 1–10.
- [33] P. T. Callaghan, in *Principles of Nuclear Magnetic Resonance Microscopy*, Clarendon, Oxford, **1993**, p.449-454
- [34] A. Botana, J. A. Aguilar, M. Nilsson, G. A. Morris, *Journal of Magnetic Resonance* **2011**, *208*, 270–278.
- [35] J. L. Guest, *Advances in Diffusion-Ordered Spectroscopy*, Université of Manchester, **2021**.
- [36] M. Nilsson, M. Khajeh, A. Botana, M. A. Bernstein, G. A. Morris, *Chem. Commun.* **2009**, 1252.
- [37] M. Oikonomou, J. Asencio-Hernández, A. H. Velders, M.-A. Delsuc, *J. Magn. Reson.* **2015**, *258*, 12–16.
- [38] M. Urbaniaczyk, D. Bernin, A. Czuroń, K. Kazimierzczuk, *Analyst* **2016**, *141*, 1745–1752.
- [39] M. Nilsson, *J. Magn. Reson.* **2009**, *200*, 296–302.
- [40] L. Castañar, G. D. Poggetto, A. A. Colbourne, G. A. Morris, M. Nilsson, *Magn Reson Chem* **2018**, *56*, 546–558.



## Entry for the Table of Contents



We describe a fast and flow compatible diffusion NMR experiment, that makes it possible to collect accurate diffusion data for samples flowing at up to 3 ml/min. We use it to monitor the synthesis of a Schiff base with a flow-tube with a time resolution of approximately 2 minutes. The one-shot flow-compatible diffusion NMR described here open many avenues for reaction monitoring applications.